Increased expression levels of inflammatory cytokines and adhesion molecules in lipopolysaccharide-induced acute inflammatory *apoM*$^{-/-}$ mice

YUANPING SHI[1], HONGYAO LIU[2], HONG LIU[2], YANG YU[1], JUN ZHANG[1], YANFEI LI[2], GUANGHUA LUO[1], XIAOYING ZHANG[2] and NING XU[3]

[1]Comprehensive Laboratory, Changzhou Key Laboratory of Individualized Diagnosis and Treatment Associated with High Technology Research; [2]Department of Cardiothoracic Surgery, The Third Affiliated Hospital of Soochow University, Changzhou, Jiangsu 213003, P.R. China; [3]Section of Clinical Chemistry and Pharmacology, Institute of Laboratory Medicine, Lund University, SE-221 85 Lund, Sweden

Received August 14, 2019; Accepted April 23, 2020

DOI: 10.3892/mmr.2020.11426

Abstract. Apolipoprotein M (apoM) may serve a protective role in the development of inflammation. Nuclear factor-κB (NF-κB) and its downstream factors (including a number of inflammatory cytokines and adhesion molecules) are essential for the regulation of inflammatory processes. In the present study, the importance of apoM in lipopolysaccharide (LPS)-induced acute inflammation and its potential underlying mechanisms, were investigated using an apoM-knockout mouse model. The levels of inducible nitric oxide synthase (iNOS), NF-κB, interleukin (IL)-1β, intercellular adhesion molecule 1 (ICAM-1) and vascular cell adhesion protein 1 (VCAM-1) were detected using reverse transcription-quantitative PCR and western blotting. The serum levels of IL-6 and IL-10 were detected using Luminex technology. The results demonstrated that the protein levels of iNOS, NF-κB, IL-1β, ICAM-1 and VCAM-1 were significantly increased in *apoM*$^{-/-}$ mice compared with those in *apoM*$^{+/+}$ mice. In addition, two-way ANOVA revealed that the interaction between apoM and LPS had a statistically significant effect on a number of factors, including the mRNA expression levels of hepatic iNOS, NF-κB, IL-1β, ICAM-1 and VCAM-1. Notably, the effects of apoM and 10 mg/kg LPS on the levels of IL-6 and IL-10 were the opposite of those induced by 5 mg/kg LPS, which could be associated with the dual anti- and pro-inflammatory effects of IL-6 and IL-10. Collectively, the results of the present study revealed that apoM is an important regulator of inflammatory cytokine and adhesion molecule production in LPS-induced inflammation, which may consequently be associated with the severity of inflammation. These findings indicated that the anti-inflammatory effects of apoM may partly result from the inhibition of the NF-κB pathway.

Correspondence to: Dr Xiaoying Zhang, Department of Cardiothoracic Surgery, The Third Affiliated Hospital of Soochow University, 185 Juqian Street, Changzhou, Jiangsu 213003, P.R. China
E-mail: zhangxy6689996@163.com

Dr Ning Xu, Section of Clinical Chemistry and Pharmacology, Institute of Laboratory Medicine, Lund University, Klinikgatan 19, SE-221 85 Lund, Sweden
E-mail: ning.xu@med.lu.se

Abbreviations: ApoM, apolipoprotein M; HDL, high-density lipoprotein; ICAM-1, intercellular adhesion molecule-1; IL, interleukin; iNOS, inducible nitric oxide synthase; LPS, lipopolysaccharide; NF-κB, nuclear factor-κB; RT-qPCR, reverse transcription-quantitative PCR; VCAM-1, vascular cell adhesion molecule-1

Key words: lipopolysaccharide, apolipoprotein M, pro-inflammatory cytokines, anti-inflammatory cytokines, adhesion molecules

Introduction

Apolipoprotein M (apoM) was discovered by Xu and Dahlback in 1999 (1). It is predominantly expressed in the liver and kidney, but also weakly expressed in colorectal tissues, and is a constituent of plasma high-density lipoproteins (HDLs) (2). As a component of HDLs, apoM is of vital importance for preβ-HDL formation in reverse cholesterol transport (3), and is suspected to be involved in anti-inflammation-associated atherogenic inhibition (4). A reduction in plasma apoM has been demonstrated in obese patients with sepsis and systemic inflammatory response syndrome (5). Additionally, apoM mRNA expressions levels have been revealed to be regulated by a number of inflammatory mediators (including platelet-activating factors) *in vivo* and/or *in vitro* (6,7). Other studies have revealed that the level of apoM is markedly correlated with that of inflammatory factors and adhesion molecules *in vitro* (5,8). Notably, the human apoM gene is located at the major histocompatibility complex class III region of chromosome 6 (chromosome 17 in mice); this region also contains a number of other genes associated with immune and inflammatory responses (9). Previous studies have demonstrated that

apoM attenuates lipopolysaccharide (LPS)-associated acute lung injury and that the number of splenic $CD4^+$ T-lymphocytes is decreased in *apoM*$^{-/-}$ mice (10,11). These studies indicated that apoM may be involved in immune and inflammatory responses *in vivo*.

Although the relationship between apoM and cytokines associated with the inflammatory response has previously been identified (5,8,12,13), the majority of these investigations were carried out *in vitro* or are clinical case studies, thus the regulatory mechanism of apoM remains to be elucidated. Nuclear factor-κB (NF-κB) is a classic member of the Rel family of transcription factors that regulates a variety of cellular functions, including inflammatory, innate and adaptive immune responses, cell proliferation and development (14,15). In fact, NF-κB can regulate the downstream expression of pro-inflammatory genes and protein adhesion molecules, including interleukin (IL)-1β, IL-6, intercellular adhesion molecule-1 (ICAM-1) and vascular cell adhesion molecule-1 (VCAM-1) (8,16,17). Conversely, the primary function of IL-10 is to inhibit the macrophage-associated generation of cytokines and chemokines, by inhibiting the activation of NF-κB and other related molecules (18).

The correlation between the expression levels of apoM and IL-10 has rarely been directly studied and the upstream and downstream effects of the association between NF-κB and IL-10 were previously unclear. To clarify the underlying mechanisms of apoM in inflammation, an acute inflammatory model of wild-type (*apoM*$^{+/+}$) and apoM deficient (*apoM*$^{-/-}$) mice was previously established (10,11). Preliminary experiments in the present study confirmed the establishment of the inflammatory model following LPS administration and that the expression levels of iNOS, NF-κB, ICAM-1, VCAM-1, IL-1β, IL-6 and the multifunctional cytokine IL-10 were increased in *apoM*$^{-/-}$ and *apoM*$^{+/+}$ mice. Furthermore, the expression levels of pro-and anti-inflammatory factors, as well as adhesion molecules were compared in the presence and absence of apoM. The interaction between apoM and LPS, and the subsequent effects on cytokine release, were also assessed.

Materials and methods

Generation of apoM-deficient mice. C57BL/6 *apoM*$^{-/-}$ mice were generated by homologous recombination at the Model Animal Research Center of Nanjing University (China) as previously described (10). A total of 36 male C57BL/6 *apoM*$^{+/+}$ and *apoM*$^{-/-}$ mice, aged 6-8 weeks and weighing ~25 g were housed in a specific pathogen-free animal experiment center at Soochow University. Food and water was provided *ad libitum*, and the conditions for a regular and stress-free life period were provided, including moderate temperature (20-25˚C), standard 12-h light/dark cycle and suitable relative humidity (55-60%).

Animals and experimental design. In the present study, experimental procedures involving animals conformed to the Jiangsu Laboratory Animal Management Ordinance and were approved by the Ethics Committee of the Third Affiliated Hospital of Soochow University. A total of 18 male *apoM*$^{+/+}$ and 18 male *apoM*$^{-/-}$ mice were divided into the following three groups: i) Saline group (control)-receiving intraperitoneal (i.p.) injections of 0.9% saline (100 µl, pyrogen-free; n=6); ii) 5 mg/kg LPS group-receiving i.p. injections of LPS (100 µl, 5 mg/kg; *Escherichia coli* serotype O111:B4; Sigma-Aldrich; Merck KGaA; MO; n=6); and iii) 10 mg/kg LPS group-receiving i.p. injections of LPS (100 µl, 10 mg/kg; n=6) (10,11,19). The mice were randomly assigned to receive three i.p. injections, once every 24 h and were sacrificed by cervical dislocation 24 h after the third injection. Blood and liver tissue samples were collected for further, immediate experimentation. To separate the serum, whole blood was left for ≥30 min at room temperature to allow coagulation, centrifuged at 1,000 x g for 10 min at room temperature and subsequently cryopreserved at -80˚C. The sera were used to detect serum iNOS, NF-κB, IL-1β, IL-6 and IL-10 levels and the liver tissue samples were used to detect iNOS, NF-κB, IL-1β, ICAM-1 and VCAM-1 expression levels.

Genotype identification of apoM knockout mice

Mouse DNA extraction. The tail tip of each mouse (~0.5 cm) was processed using the Ezup Column Animal Genomic DNA Extraction kit (Sangon Biotech Co., Ltd.) according to the manufacturer's protocol. Specimens with absorbance values ($A_{260/280\ nm}$) of 1.8-1.9 were stored at -20˚C and used for subsequent experimentation.

Primer and probe design. The base sequences of apoM (NC_000083.6, https://www.ncbi.nlm.nih.gov/nuccore/NC_000083.6)andLox-Neo-LoxP(NC_000086.7, https://www.ncbi.nlm.nih.gov/nuccore/NC_000086.7) were obtained from GenBank (NCBI). The PCR primers and probe sets (Table I) were designed using Primer Premier 5.00 (Premier Biosoft International) and synthesized by Sangon Biotech Co., Ltd. The mouse *apoM*$^{+/+}$ probe was labeled with a fluorescent 6-carboxyfluorescein (6-FAM) group and the *apoM*$^{-/-}$ probe was labeled with a 3H-II phthalocyanine dye (CY5) at the 5'-end, as previously described (20).

Duplex fluorescence real-time PCR for mouse genotype identification. Duplex fluorescence real-time PCR was performed using the LightCycler 480 II PCR system (Roche Diagnostics GmbH) to enable dual-channel fluorescence detection. The amplification reactions contained 2.5 µl 10X PCR Buffer (including Mg^{++}), 2 µl 2.5 mM dNTPs, 0.1 µl of each primer and probe (100 µM; Table I), 0.125 µl Taq polymerase (5 U/µl), 2 µl template (replaced by water in the no template controls) and nuclease-free water up to a final volume of 25 µl. The thermocycling conditions were: 95˚C for 3 min, 40 cycles at 95˚C for 10 sec and 60˚C for 15 sec and 40˚C for 30 sec. Fluorescence signals were acquired at 60˚C and detected using the FAM (465-510 nm, *apoM*$^{+/+}$ mice) and CY5 (618-660 nm, *apoM*$^{-/-}$ mice) channels. When the Ct value was ≤35, PCR amplification was considered to be successful; when the Ct value was >40, or there was no value, the detection result was considered to be negative; when a Ct value >35 and <40 was obtained, a retest was recommended. A single *apoM*$^{+/+}$ and *apoM*$^{-/-}$ PCR product were selected to verify the methodology (cloning and sequencing, performed by Shanghai Biotech Co., Ltd.), as previously described (20).

Hematoxylin and eosin (H&E) Staining of hepatic tissues. Hepatic samples were fixed in 10% formalin for 24 h at room temperature and then embedded in paraffin. Hepatic sections were cut into 5-µm-thick slices and used for H&E staining

Table I. Mouse genotype identification primers and probes for dual probe PCR.

Name	Primer/probe	Sequence (5'-3')	Product length (base pairs)
apoM$^{+/+}$ mouse	Forward primer	CGGAAGTGGACATACCGATTG	105
	Reverse primer	AAACGGCTAAGGGAGACGAGA	
	Probe	FAM-CTGAAGGTTGGTTCCCACCAGCCC-BHQ1	
apoM$^{-/-}$ mouse	Forward primer	GCTCCTGCCGAGAAAGTATCC	98
	Reverse primer	CGATGTTTCGCTTGGTGGTC	
	Probe	CY5-TGCAATGCGGCGGCTGCATACGCT-BHQ2	

according to the established method (21). All slides were examined under an inverted microscope (Olympus IX73, magnification, x200) by an experienced pathologist.

Reverse transcription-quantitative (RT-q) PCR quantification of mRNA expression levels of iNOS, NF-κB, IL-1β, ICAM-1 and VCAM-1 in liver tissues. Total RNA was extracted from liver tissues using an RNA purification kit (Shanghai Shenergy Biocolor Bioscience and Technology Co., Ltd.) according to the manufacturer's instructions. The quality and quantity of the RNA were determined by spectrophotometry (Eppendorf) at 260/280 nm. A total of 2 μg RNA was reverse-transcribed using the RevertAid First-strand cDNA Synthesis kit per the manufacturer's protocol (Thermo Fisher Scientific, Inc.); the PCR primer and probe sets (listed in Table II) were designed using Primer Premier 5.00 (Premier Biosoft International) and synthesized by Sangon Biotech Co., Ltd. GAPDH was used as the reference control. The amplification reactions contained (SNBC Bioon, Inc.) 2.5 μl 10X PCR buffer (including Mg^{++}), 2 μl 2.5 mM dNTPs, 0.1 μl of each primer (100 μM), 0.05 μl probe (100 μM), 0.125 μl 5 U/μl Taq polymerase, 2 μl template (replaced by water in the no template controls) and nuclease-free water to a final volume of 25 μl. The thermocycling conditions were: 95˚C for 3 min, followed by 40 cycles at 95˚C for 5 sec and 60˚C for 15 sec. The relative mRNA expression level was determined using the $2^{-\Delta\Delta Cq}$ method (22).

Determination of the protein expression levels of iNOS, NF-κB, IL-1β, ICAM-1 and VCAM-1 using western blotting. Hepatic protein samples were extracted using a total protein extraction kit (BestBio Biotechnology) and protein quantified using the BCA method (BestBio Biotechnology). Serum samples were diluted (1:25) and loaded onto 8% SDS-page gels and subsequently transferred onto 0.45 μm PVDF membranes (EMD Millipore). The membranes were blocked in 1X PBST containing 3% bovine serum albumin (Multi Sciences, Inc.) for 2 h at room temperature. The membranes were incubated with primary antibodies against iNOS (1:300; cat. no. 18985-1-AP; ProteinTech Group, Inc.), NF-κB (1:1,000; cat. no. 8242; Cell Signaling Technology, Inc.), IL-1β (1:1,000; cat. no. 12242; Cell Signaling Technology, Inc.), ICAM-1 (1:300; cat. no. sc-18853; Santa Cruz Biotechnology, Inc.), VCAM-1 (1:300; cat. no. sc-13160; Santa Cruz Biotechnology, Inc.), GAPDH (1:3,000; cat. no. ARG10112, Arigo Biolaboratories Corp.) and Transferrin (1:500; cat. no. 17435-1-AP; ProteinTech Group, Inc.) overnight at 4˚C. Then, the membranes were incubated with secondary antibodies of HRP-conjugated Affinipure Goat Anti-Mouse IgG (H+L) (1:3,000; cat. no. SA00001-1, ProteinTech Group, Inc.) and HRP-conjugated Affinipure Goat Anti-Rabbit IgG (H+L) (1:3,000; cat. no. SA00001-2, ProteinTech Group, Inc.) for 1 h at room temperature. The protein blots were observed using an ECL chemiluminescent kit (ECL plus; Thermo Fisher Scientific, Inc.) and the gray values of the bands were measured using Clinx ChemiCapture 3300 (Shanghai Clinx Science Instruments Co., Ltd.) and Quantity One software v4.6.2 (Bio-Rad Laboratories, Inc.).

Detection of serum iNOS. Serum iNOS was detected using an NOS typing assay kit (cat. no. A014-1; Nanjing Jiancheng Bioengineering Institute) according to the manufacturer's protocol. The absorbance was measured at a wavelength of 530 nm and NOS activity was calculated based on the absorbance value.

Detection of serum ICAM-1 and VCAM-1. Serum ICAM-1 and VCAM-1 were detected using enzyme-linked immunosorbent assay kits (cat. nos. H065 and H066; Nanjing Jiancheng Bioengineering Institute) according to the manufacturer's protocols. The absorbance was measured at a wavelength of 450 nm.

Determination of IL-6 and IL-10 expression levels by Luminex assay. Prior to the bioassay, samples were thawed on ice and homogenized by vortexing for 10 sec, followed by centrifugation at 1,000 x g for 10 min at room temperature. The concentrations of serum IL-6 and IL-10 were detected using a Luminex 200 system (Luminex Corporation) with the MILLIPLEX® Map kit and the Human Magnetic Bead MAPmate™ Buffer kit (EMD Millipore). The wells of the standard, control and background samples were assayed in duplicate and standard curves were extended down to <1.0 pg/ml. The assays were performed using a Luminex 200 multiplexing instrument (Luminex Corporation) according to the manufacturer's instructions, at 4˚C with shaking 1,000 rpm for 16 h on a plate shaker (Eppendorf) and using a hand-held magnetic block for each wash step. In summary, each well of the 96-well microtiter plates was pre-wetted with wash buffer, prior to the addition of 25 μl sample and 25 μl of the appropriate buffer (Assay Buffer, Standard, or Control 1 or 2) to the background, standard and control wells (according to the standard curve). The plates were then incubated with 25 μl pre-mixed antibody-immobilized beads overnight on an orbital shaker at 4˚C. The plates were washed

Table II. Primers and fluorescent probes for reverse transcription-quantitative PCR.

Name	Primer/probe	Sequence (5'-3')
iNOS	Forward primer	TGCCACGGACGAGACGG
	Reverse primer	TGTTGCTGAACTTCCAGTCATTGT
	Probe	FAM-AGAGATTGGAGGCCTTGTGTCAGCC-TAMRA
NF-κB	Forward primer	GAGAAGAACAAGAAATCCTACCCAC
	Reverse primer	TCCATTTGTGACCAACTGAACG
	Probe	FAM-CAACTATGTGGGGCCTGCAAAGGTT-TAMRA
IL-1β	Forward primer	GCAGGCAGTATCACTCATTGTGG
	Reverse primer	GAGTCACAGAGGATGGGCTCTTC
	Probe	FAM-TGGAGAAGCTGTGGCAGCTACCTGTGT-TAMRA
ICAM-1	Forward primer	ATCACCGTGTATTCGTTTCCG
	Reverse primer	GTGAGGTCCTTGCCTACTTGCT
	Probe	FAM-AGTGTGGAGCTGAGACCTCTGCCAGCCT-TAMRA
VCAM-1	Forward primer	CTGAACCCAAACAGAGGCAGA
	Reverse primer	GGTATCCCATCACTTGAGCAGG
	Probe	FAM-CATCTGGGTCAGCCCCTCTCCTATACTAGA-TAMRA
GAPDH	Forward primer	TCTTGTGCAGTGCCAGCCT
	Reverse primer	TGAGGTCAATGAAGGGGTCG
	Probe	FAM-AGGTCGGTGTGAACGGATTTGGC-TAMRA

iNOS, inducible nitric oxide synthase; NF-κB, nuclear factor-κB; IL, interleukin; ICAM-1, intercellular adhesion molecule 1; VCAM-1, vascular cell adhesion protein 1.

twice with wash buffer and 25 μl biotinylated detector antibody was added to each well and incubated for 1 h at room temperature. Without further washing, 25 μl streptavidin-phycoerythrin solution was added to each well and the plates were incubated for 30 min at room temperature on a plate shaker, protected from direct light. Prior to analysis, the beads were washed twice in wash buffer and resuspended in 150 μl/well Luminex sheath fluid.

Statistical analysis. The data are expressed as the means ± standard error or the mean. Statistical analysis was conducted using Prism software, version 6.0 (GraphPad Software, Inc.). Comparisons between two groups were statistically evaluated using the Mann-Whitney test and those between three groups were analyzed using Ordinary one-way ANOVA followed by Tukey's post hoc test. Cross interaction was analyzed by two-way ANOVA. $P<0.05$ was considered to indicate a statistically significant difference.

Results

Analysis of PCR amplification curves for mouse genotype identification. The PCR amplification curves were consistent with the effective amplification results (Ct value ≤35). Mice with a significant 's' type amplification curve in the FAM channel and no amplification in the CY5 channel were identified as *apoM* $^{+/+}$. Mice with a significant 's' type amplification curve in the CY5 channel and no amplification in the FAM channel were identified as *apoM*$^{-/-}$. Mice with a prominent 'S' type amplification curve in both channels were apoM heterozygous (*apoM*$^{+/-}$; Fig. S1).

PCR product cloning and sequencing alignment. An *apoM*$^{+/+}$ and an *apoM*$^{-/-}$ PCR product were selected for cloning and sequencing (performed by Shanghai Biotech Co., Ltd.). Sequence alignment indicated that the sequences of the *apoM*$^{+/+}$ and *apoM*$^{-/-}$ PCR products in the subsequent recombinant plasmids completely matched those of their respective sequences (Fig. S2).

Confirmation of the successful establishment of the inflammatory model following LPS administration. Following the administration of 10 mg/kg LPS to the *apoM*$^{-/-}$ and *apoM*$^{+/+}$ mice, H&E staining revealed significant inflammatory pathological changes in the liver, including the infiltration of inflammatory cells into the liver portal area. The reaction to LPS treatment was more pronounced in *apoM*$^{-/-}$ mice than in *apoM*$^{+/+}$ mice; the degree of inflammatory cell exudate was greater and the number of Kupffer cells was increased (Fig. 1A-D). As a clear indicator of inflammation, the mRNA and protein levels of iNOS were significantly increased in the liver and serum of LPS-treated mice, especially in the *apoM*$^{-/-}$ group (Fig. 1E-J; $P<0.05$).

Effects of LPS and/or apoM on NF-κB and IL-1β expression levels in apoM$^{-/-}$ *and apoM*$^{+/+}$ *mice*. There were no significant differences in the expression levels of NF-κB and IL-1β between the *apoM*$^{-/-}$ and *apoM*$^{+/+}$ mice of the saline control group. Following the administration of 10 mg/kg LPS, the expression levels of NF-κB mRNA increased 3.42- ($P<0.05$) and 1.74-fold ($P<0.05$) and those of IL-1β mRNA increased 6.18- ($P<0.01$) and 4.84-fold ($P<0.05$), in the *apoM*$^{-/-}$ and *apoM*$^{+/+}$ mice, respectively, when compared with the saline

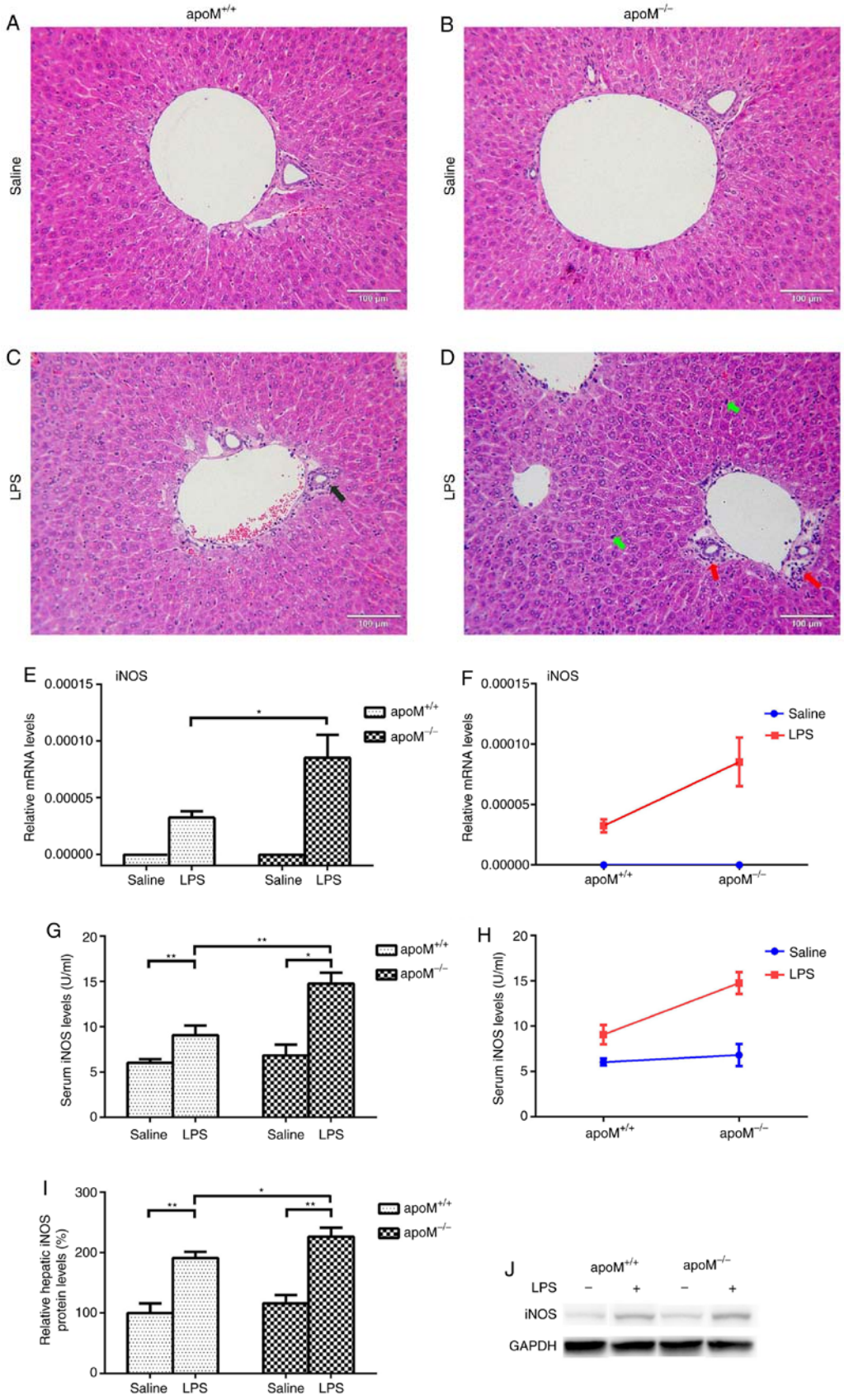

Figure 1. Confirmation of the successful establishment of an LPS-induced inflammatory mouse model. Mice (n=6 per group) were randomly assigned to receive intraperitoneal injections of 0.9% saline (100 μl) or LPS (10 mg/kg in 100 μl saline) 3 times, once every 24 h. (A-D) Hematoxylin and eosin staining of mouse livers. The black arrow indicates a small number of inflammatory cells in the liver portal area of an *apoM*$^{+/+}$ mouse treated with LPS. The red arrow indicates a large number of inflammatory cells in the liver portal area of an LPS-treated *apoM*$^{-/-}$ mouse. Green arrows indicate an increased number of Kupffer cells in the liver of an LPS-treated *apoM*$^{-/-}$ mouse. Liver sections, 5 μm; magnification, x200; scale bar=100 μm. (E, G and I) Effects of LPS and/or apoM on hepatic and serum expression levels of iNOS in *apoM*$^{-/-}$ and *apoM*$^{+/+}$ mice. (F and H) Effects of cross interaction between apoM and LPS on iNOS expression levels. (J) Western blot analysis. Data are presented as the means ± standard error or the mean. *P<0.05 and **P<0.01. LPS, lipopolysaccharide; apoM, apolipoprotein M; iNOS, inducible nitric oxide synthase.

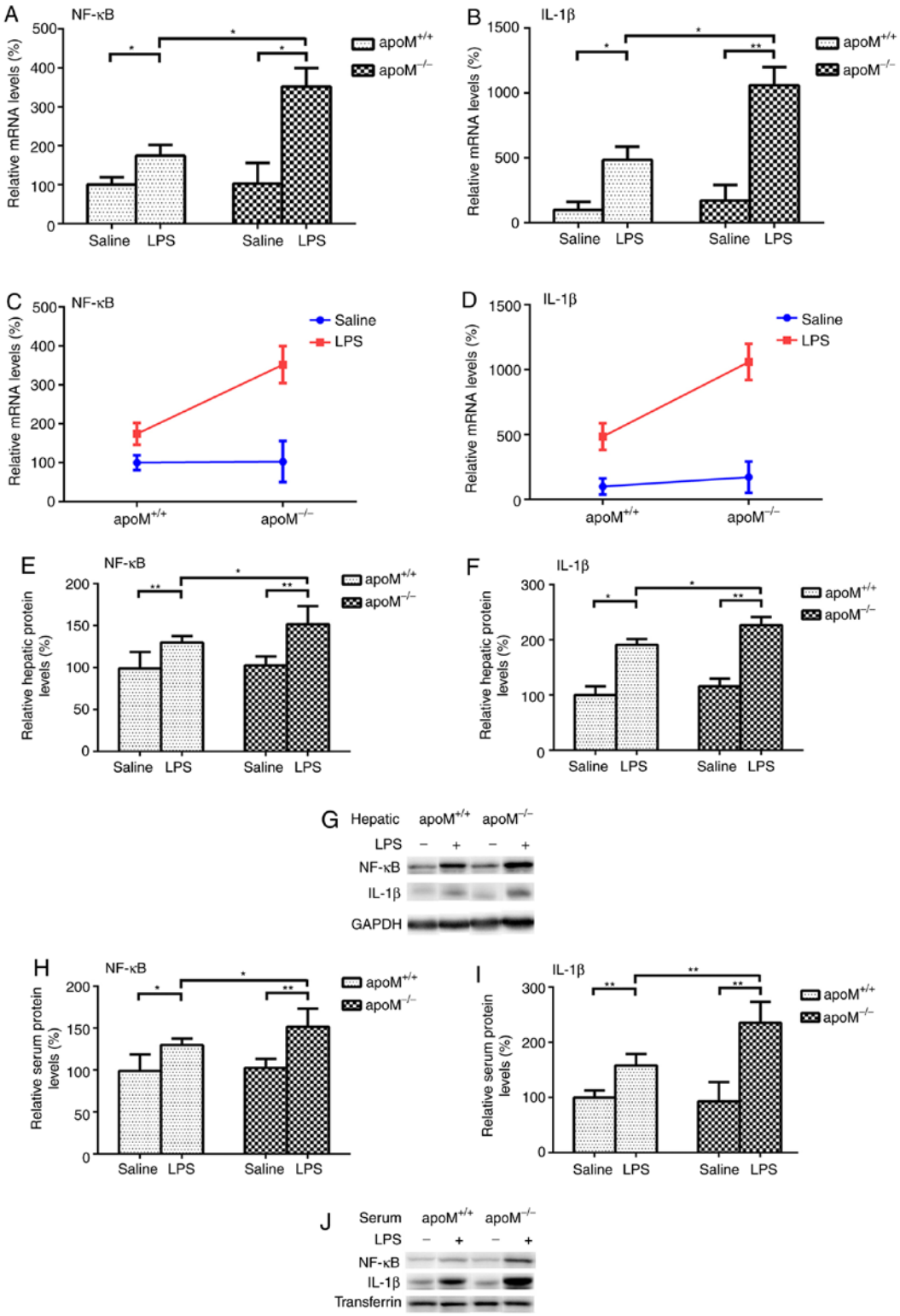

Figure 2. Effects of LPS and/or apoM on NF-κB and IL-1β expression levels. Mice (n=6 per group) were randomly assigned to receive intraperitoneal injections of 0.9% saline (100 μl) or LPS (10 mg/kg in 100 μl saline) 3 times, once every 24 h. (A and B) Effects of LPS and/or apoM on the hepatic mRNA expression levels of NF-κB and IL-1β in *apoM*$^{-/-}$ and *apoM*$^{+/+}$ mice. (C and D) Effects of cross interaction between apoM and LPS on NF-κB and IL-1β mRNA expression levels. (E, F, H and I) Effects of LPS and/or apoM on hepatic and serum protein expression levels of NF-κB and IL-1β in *apoM*$^{-/-}$ and *apoM*$^{+/+}$ mice. (G and J) Western blot analysis. Data are presented as the means ± standard error or the mean. *P<0.05 and **P<0.01. LPS, lipopolysaccharide; apoM, apolipoprotein M; NF-κB, nuclear factor-κB; IL, interleukin.

group (Fig. 2A and B). Following LPS treatment, the mRNA expression levels of hepatic NF-κB and IL-1β in the *apoM*$^{-/-}$ mice were 2.02 and 2.19 times that of those in the *apoM*$^{+/+}$ mice (Fig. 2A and B; P<0.05). Two-way ANOVA revealed that the effects of apoM and LPS interaction on the expression levels of hepatic NF-κB and IL-1β mRNA were statistically significant (Fig. 2C and D; P<0.05). NF-κB and IL-1β protein expression levels were also significantly increased in the liver

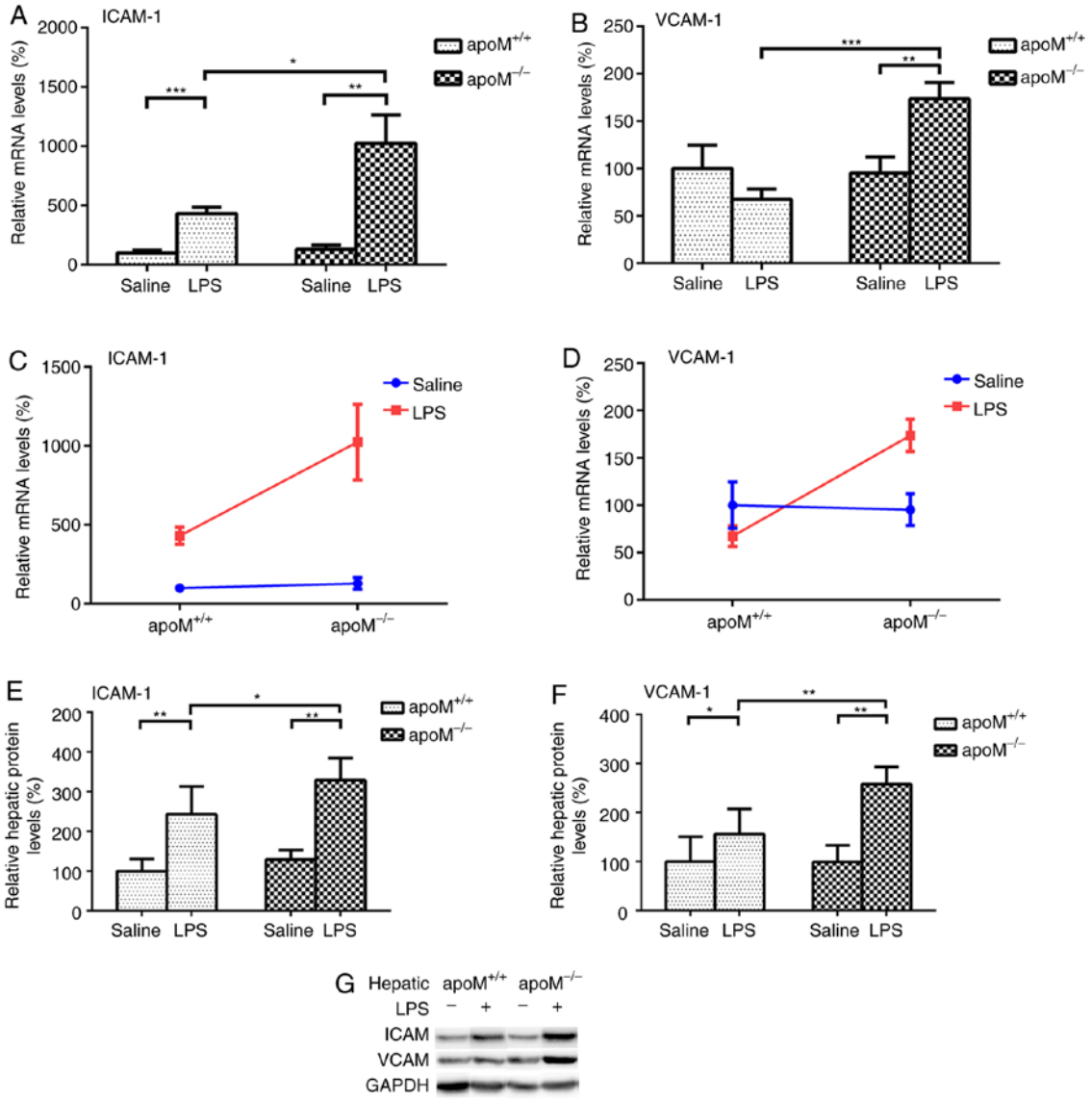

Figure 3. Effects of LPS and/or apoM on ICAM-1 and VCAM-1 expression levels. Mice (n=6 per group) were randomly assigned to receive intraperitoneal injections of 0.9% saline (100 μl) or LPS (10 mg/kg in 100 μl saline) 3 times, once every 24 h. (A and B) Effects of LPS and/or apoM on hepatic mRNA expression levels of ICAM-1 and VCAM-1 in *apoM*$^{-/-}$ and *apoM*$^{+/+}$ mice. (C and D) Effect of cross interaction between apoM and LPS on ICAM-1 and VCAM-1 mRNA expression levels. (E and F) Effects of LPS and/or apoM on hepatic protein expression levels of ICAM-1 and VCAM-1 in *apoM*$^{-/-}$ and *apoM*$^{+/+}$ mice. (G) Western blot analysis. Data are presented as the means ± standard error or the mean. *P<0.05, **P<0.01 and ***P<0.001. LPS, lipopolysaccharide; apoM, apolipoprotein M; ICAM-1, intercellular adhesion molecule 1; VCAM-1, vascular cell adhesion protein 1.

and serum of LPS-treated mice, particularly in the *apoM*$^{-/-}$ group (Fig. 2E-J; P<0.05).

Effects of LPS and/or apoM on ICAM-1 and VCAM-1 expression levels in apoM$^{-/-}$ *and apoM*$^{+/+}$ *mice*. There were no significant differences in the expression levels of ICAM-1 and VCAM-1 between *apoM*$^{-/-}$ and *apoM*$^{+/+}$ mice in the saline control group. Compared with this group, the injection of 10 mg/kg LPS resulted in a 7.95- (P<0.01) and 4.30-fold (P<0.001) increase in the expression levels of ICAM-1 mRNA in *apoM*$^{-/-}$ and *apoM*$^{+/+}$ mice, respectively (Fig. 3A); the expression level of VCAM-1 increased 1.82-fold (Fig. 3B; P<0.01) in the *apoM*$^{-/-}$ mice, though there was no significant difference in VCAM-1 expression in the *apoM*$^{+/+}$ mice. Additionally, LPS administration increased the mRNA expression levels of hepatic ICAM-1 and VCAM-1 in the *apoM*$^{-/-}$ mice to 2.38 and 2.57 times that of the *apoM*$^{+/+}$ mice (Fig. 3A and B; P<0.05 and P<0.001, respectively). Two-way ANOVA revealed that the effects of the apoM and LPS interaction on hepatic ICAM-1 and VCAM-1 mRNA expression levels was statistically significant (Fig. 3C and D; P<0.05). ICAM-1 and VCAM-1 protein levels were also significantly increased in the livers of LPS-treated mice, especially those in the *apoM*$^{-/-}$ group (Fig. 3E-G; P<0.05). The protein mass of ICAM-1 and VCAM-1 in serum were not detected using western blotting and enzyme-linked immunosorbent assay.

Effects of LPS and/or apoM on serum cytokine levels of IL-6 and IL-10 in apoM$^{-/-}$ *and apoM*$^{+/+}$ *mice*. Following treatment with LPS, the serum IL-6 and IL-10 levels were significantly increased in both *apoM*$^{+/+}$ and *apoM*$^{-/-}$ mice (Fig. 4A and B; P<0.001). Furthermore, serum IL-6 and IL-10 levels were

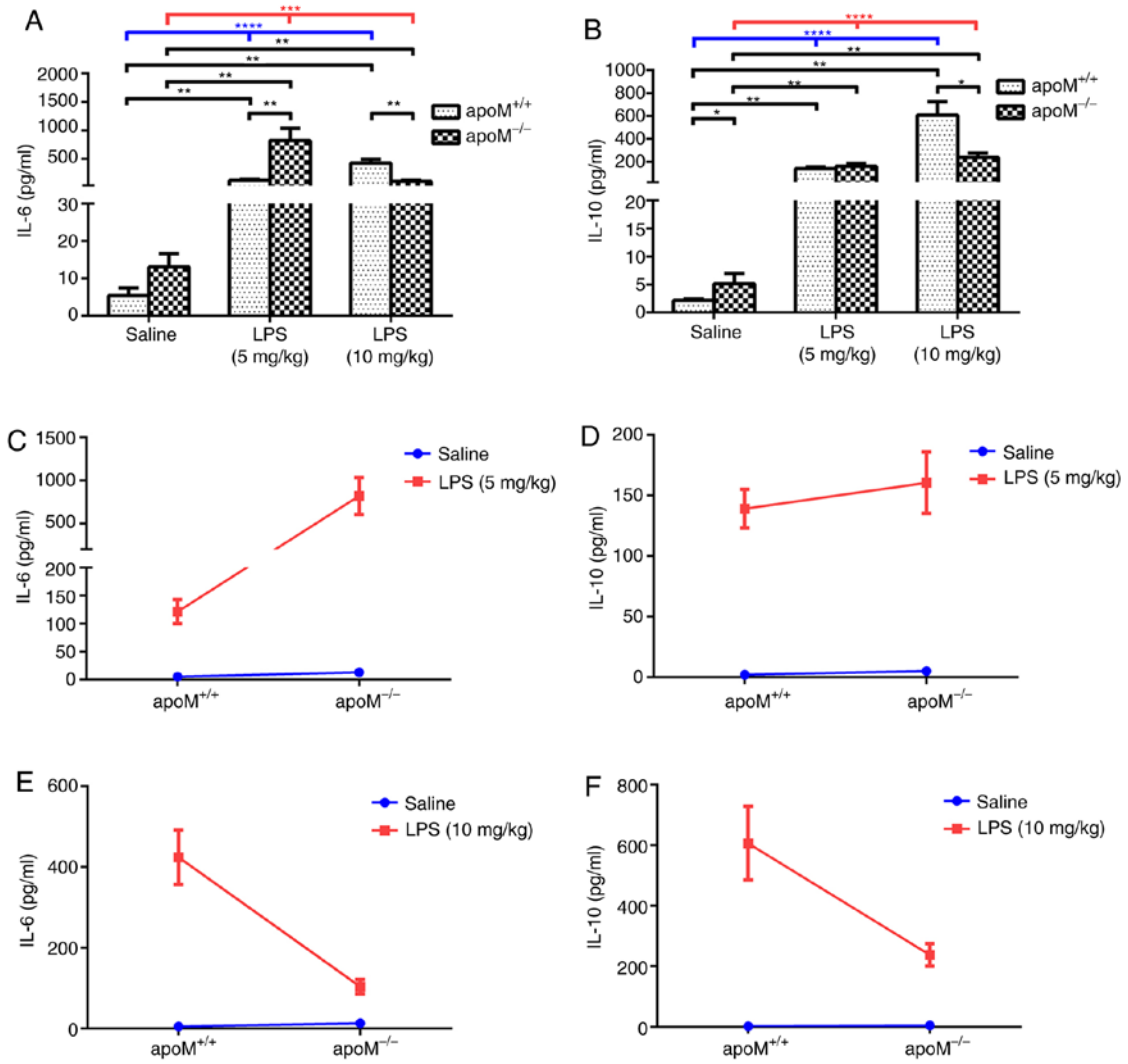

Figure 4. Effects of LPS and/or apoM on serum IL-6 and IL-10 levels. Mice (n=6 per group) were randomly assigned to receive intraperitoneal injections of 0.9% saline (100 μl) or LPS (5 or 10 mg/kg in 100 μl saline) 3 times, once every 24 h. (A and B) Effects of LPS and/or apoM on the levels of serum IL-6 and IL-10 in *apoM*$^{-/-}$ and *apoM*$^{+/+}$ mice. (C-F) Effects of cross interaction between apoM and LPS on serum IL-6 and IL-10 levels in 5- and 10 mg/kg-LPS groups. Data are presented as the means ± standard error or the mean. *P<0.05, **P<0.01, ***P<0.001 and ****P<0.0001. LPS, lipopolysaccharide; apoM, apolipoprotein M; IL, interleukin.

increased in the LPS group, compared with the saline group (Fig. 4A and B; P<0.01), although there was no significant difference between the serum IL-6 levels of the *apoM*$^{+/+}$ and *apoM*$^{-/-}$ mice in the saline group. After a 5 mg/kg injection of LPS, the serum levels of IL-6 in the *apoM*$^{-/-}$ mice were considerably higher than those in the *apoM*$^{+/+}$ mice (P<0.01). However, after 10 mg/kg LPS, the serum levels of IL-6 in the *apoM*$^{-/-}$ mice were lower than those in the apoM$^{+/+}$ mice (Fig. 4A; P<0.01).

The levels of serum IL-10 in the *apoM*$^{-/-}$ mice were higher than those in the *apoM*$^{+/+}$ mice of the saline group (P<0.05), but no significant difference was observed between the *apoM*$^{+/+}$ and *apoM*$^{-/-}$ mice in the 5 mg/kg LPS-treatment group. However, the serum IL-10 levels in *apoM*$^{-/-}$ mice were notably lower than those in the *apoM*$^{+/+}$ mice following treatment with 10 mg/kg LPS (Fig. 4B; P<0.05). Furthermore, two-way ANOVA revealed that the effects of apoM and LPS interaction on serum IL-6 levels in the 5 mg/kg LPS group were statistically significant (Fig. 4C; P<0.01), whilst there were no significant differences in the levels of IL-10 (Fig. 4D). The effects of the apoM and LPS interaction on serum IL-6 and IL-10 levels in the 10 mg/kg LPS group were also statistically significant (Fig. 4E and F; P<0.001 and P<0.01, respectively). Interaction analyses between apoM and LPS in the two different dose groups indicated that an increase in LPS resulted in a decrease in IL-6 and IL-10 serum expression levels in *apoM*$^{-/-}$ mice, compared with *apoM*$^{+/+}$ mice.

Discussion

Inflammation is predominantly involved in the host defense against infection and cellular damage (23,24). It can widely occur in vascularized tissues and is closely associated with the occurrence and development of tumors and diseases such as atherosclerosis and diabetes (25). Various inflammatory factors and adhesion molecules serve important roles in the development of inflammation (23,26). In recent years, the anti-inflammatory properties of apoM have received increasing attention, with a number of studies revealing its

ability to inhibit inflammation in atherogenesis, chronic infection, pneumonia and bowel cancer (2,11,27,28). However, the effects of apoM on the expression of adhesion molecules during inflammation, particularly the multifunctional cytokine IL-10, are less well studied and to date, the underlying mechanisms remained unknown. In the present study, apoM was revealed to significantly inhibit the expression of iNOS, NF-κB, IL-1β, ICAM-1 and VCAM-1 in an LPS-induced mouse model. Furthermore, the expression level of serum IL-6 and IL-10 was increased in mice induced with different concentrations of LPS. Notably, the effects of apoM on IL-10 and IL-6 were reversed with increasing concentrations of LPS.

Our previous study (11) demonstrated that the expression levels of IL-1β and IL-6 were significantly increased in the lung tissues of 10 mg/kg LPS-induced *apoM*$^{-/-}$mice, compared with the *apoM*$^{+/+}$ group, suggesting that apoM exerts anti-inflammatory effects in LPS-induced acute lung injury. These results also revealed that LPS treatment increased the expression levels of IL-1β, IL-6 and IL-10, and that NF-κB expression in the 10-mg/kg LPS group also increased significantly in *apoM*$^{-/-}$, compared with *apoM*$^{+/+}$ mice. However, further analysis showed that when treated with 5 mg/kg LPS, apoM inhibited the effects of LPS on IL-6, resulting in an anti-inflammatory effect. By contrast, in the 10 mg/kg LPS group, apoM promoted the effects of LPS on IL-6 and IL-10. Previous studies have revealed that IL-6 and IL-10 possess both pro- and anti-inflammatory properties (29,30). The reason may be that in the early stages, apoM retards inflammation by inhibiting the production of IL-6. In more severe cases, apoM may exert its anti-inflammatory effects by increasing the expression levels of both IL-6 and IL-10, although the specific mechanism of this inference requires further investigation.

The transcription factor NF-κB exerts protective and anti-apoptotic effects in the liver, and is considered to be a key inducible, rather than constitutively expressed regulator, of inflammation that is responsive to pro-inflammatory cytokines (31,32). Previous studies have revealed that NF-κB is a key factor regulating the expression of various genes, including IL-1β, IL-6, ICAM-1 and VCAM-1; it can be regulated by IL-10 (8,16,18) and as such, is integral to inflammatory reactions such as the immune response, smooth muscle cell proliferation and angiogenesis. A number of studies have suggested that apoM is able to inhibit the activity of NF-κB and the expression of inflammatory factors through various biological pathways, dependent or independent of sphingosine 1-phosphate (5,8,12,33-35). Gao *et al* (8) revealed that apoM reduced the expression levels of ICAM-1 and VCAM-1 by inhibiting NF-κB activity. Therefore, apoM was speculated to inhibit the expression of pro-inflammatory factors and adhesion molecules by preventing NF-κB activation, thereby exerting a protective effect against inflammation. As aforementioned, studies (18,30) have shown that the primary function of IL-10 is to inhibit the production of cytokines and chemokines in macrophages. This is achieved by inhibiting a number of inflammatory molecules, including NF-κB (18), which can also regulate the expression of IL-10 (30). To the best of the authors' knowledge, the direct upstream and downstream relationship between apoM and IL-10 has yet to be elucidated, thus, in the present study, the expression levels of IL-10 in *apoM*$^{-/-}$ mice were determined and further analyses were performed to confirm the interaction between IL-10 and apoM. Serum ICAM-1 and VCAM-1 are generally detected by enzyme-linked immunosorbent assay (36,37), but in the present study, they were not detected using western blotting and enzyme-linked immunosorbent assay, probably because their expression levels were too low.

In summary, the inflammatory response is a complex process with mutual, network-like regulation between cytokines and its regulatory balance may be associated with the development and severity of the inflammatory response. The aforementioned results indicated that apoM is involved in the regulation of inflammatory factors and adhesion molecules in acute LPS-induced inflammation. Furthermore, apoM may act by retarding the expression of inflammatory factors and adhesion molecules through the inhibition of NF-κB. These findings have expanded the network of research on inflammatory development, providing greater opportunities to treat inflammatory pathologies and suggesting that apoM may be a potential target for the clinical treatment of inflammation (particularly vascular inflammation).

Acknowledgements

Not applicable.

Funding

This study was supported by the National Natural Science Foundation of China (grant no. 81370372), the Natural Science Foundation of Jiangsu province (grant nos. BK20191158 and BK20151179) and the Jiangsu Provincial Youth Medicine Key Talent Project (grant no. QNRC2016282).

Availability of data and materials

The datasets used during the present study are available from the corresponding author upon reasonable request.

Authors' contributions

XZ, GL and NX made substantial contributions to the conception and design of the study. YS performed the experiments, analyzed the data and contributed to writing the manuscript. YY performed the genotype identification experiments. HongyL, JZ and HongL detected the inflammatory cytokines and adhesion molecule expression levels. YL analyzed the data. All authors read and approved the final version of the manuscript.

Ethics approval and consent to participate

In the present study, experimental procedures involving animals conformed to the Jiangsu Laboratory Animal Management Ordinance and were approved by the Ethics Committee of the Third Affiliated Hospital of Soochow University.

Patient consent for publication

Not applicable.

Competing interests

The authors declare that they have no competing interests.

References

1. Xu N and Dahlback B: A novel human apolipoprotein (apoM). J Biol Chem 274: 31286-31290, 1999.
2. Luo G, Zhang X, Mu Q, Chen L, Zheng L, Wei J, Berggren-Soderlund M, Nilsson-Ehle P and Xu N: Expression and localization of apolipoprotein M in human colorectal tissues. Lipids Health Dis 9: 102, 2010.
3. Feng YH, Zheng L, Wei J, Yu MM, Zhang J, Luo GH and Xu N: Increased apolipoprotein M induced by lack of scavenger receptor BI is not activated via HDL-mediated cholesterol uptake in hepatocytes. Lipids Health Dis 17: 200, 2018.
4. Wei J, Yu Y, Feng Y, Zhang J, Jiang Q, Zheng L, Zhang X, Xu N and Luo G: Negative correlation between serum levels of homocysteine and apolipoprotein M. Curr Mol Med 19: 120-126, 2019.
5. Li T, Yang L, Zhao S and Zhang S: Correlation between apolipoprotein M and inflammatory factors in obese patients. Med Sci Monit 24: 5698-5703, 2018.
6. Luo G, Shi Y, Zhang J, Mu Q, Qin L, Zheng L, Feng Y, Berggren-Söderlund M, Nilsson-Ehle P, Zhang X and Xu N: Palmitic acid suppresses apolipoprotein M gene expression via the pathway of PPARβ/δ in HepG2 cells. Biochem Biophys Res Commun 445: 203-207, 2014.
7. Ren K, Tang ZL, Jiang Y, Tan YM and Yi GH: Apolipoprotein M. Clin Chim Acta 446: 21-29, 2015.
8. Gao JJ, Hu YW, Wang YC, Sha YH, Ma X, Li SF, Zhao JY, Lu JB, Huang C, Zhao JJ, *et al*: ApoM suppresses TNF-α-induced expression of ICAM-1 and VCAM-1 through inhibiting the activity of NF-κB. DNA Cell Biol 34: 550-556, 2015.
9. Huang XS, Zhao SP, Hu M and Luo YP: Apolipoprotein M likely extends its anti-atherogenesis via anti-inflammation. Med Hypotheses 69: 136-140, 2007.
10. Wang Z, Luo G, Feng Y, Zheng L, Liu H, Liang Y, Liu Z, Shao P, Berggren-Söderlund M, Zhang X and Xu N: Decreased splenic CD4(+) T-lymphocytes in apolipoprotein M gene deficient mice. Biomed Res Int 2015: 293512, 2015.
11. Zhu B, Luo GH, Feng YH, Yu MM, Zhang J, Wei J, Yang C, Xu N and Zhang XY: Apolipoprotein M protects against lipopolysaccharide-induced acute lung injury via sphingosine-1-phosphate signaling. Inflammation 41: 643-653, 2018.
12. Frej C, Mendez AJ, Ruiz M, Castillo M, Hughes TA, Dahlbäck B and Goldberg RB: A shift in ApoM/S1P between HDL-particles in women with type 1 diabetes mellitus is associated with impaired anti-inflammatory effects of the ApoM/S1P complex. Arterioscler Thromb Vasc Biol 37: 1194-1205, 2017.
13. Ruiz M, Frej C, Holmer A, Guo LJ, Tran S and Dahlbäck B: High-density lipoprotein-associated apolipoprotein M limits endothelial inflammation by delivering sphingosine-1-phosphate to the sphingosine-1-phosphate receptor 1. Arterioscler Thromb Vasc Biol 37: 118-129, 2017.
14. Sun SC: The non-canonical NF-κB pathway in immunity and inflammation. Nat Rev Immunol 17: 545-558, 2017.
15. King KE, George AL, Sakakibara N, Mahmood K, Moses MA and Weinberg WC: Intersection of the p63 and NF-κB pathways in epithelial homeostasis and disease. Mol Carcinog 58: 1571-1580, 2019.
16. Chen KY and Wang LC: Stimulation of IL-1β and IL-6 through NF-κB and sonic hedgehog-dependent pathways in mouse astrocytes by excretory/secretory products of fifth-stage larval angiostrongylus cantonensis. Parasit Vectors 10: 445, 2017.
17. Nonaka K, Kajiura Y, Bando M, Sakamoto E, Inagaki Y, Lew JH, Naruishi K, Ikuta T, Yoshida K, Kobayashi T, *et al*: Advanced glycation end-products increase IL-6 and ICAM-1 expression via RAGE, MAPK and NF-κB pathways in human gingival fibroblasts. J Periodontal Res 53: 334-344, 2018.
18. Conti P, Kempuraj D, Kandere K, Di Gioacchino M, Barbacane RC, Castellani ML, Felaco M, Boucher W, Letourneau R and Theoharides TC: IL-10, an inflammatory/inhibitory cytokine, but not always. Immunol Lett 86: 123-129, 2003.
19. Song X, Ren Z and Zhang C: Antioxidant, anti-inflammatory and renoprotective effects of acidic-hydrolytic polysaccharides by spent mushroom compost (*Lentinula edodes*) on LPS-induced kindey injury. Int J Biol Macromol 151: 1267-1276, 2020.
20. Yang Y, Lu Z, Yun L, Li P, Jun Z, Jiang W, Miao M and Guang L: Establishment of real-time quantitative PCR method for identification of apolipoprotein M knockout mice. Chin J Clin Lab Sci 33: 3, 2015.
21. Wu BM, Liu JD, Li YH and Li J: Margatoxin mitigates CCl4induced hepatic fibrosis in mice via macrophage polarization, cytokine secretion and STAT signaling. Int J Mol Med 45: 103-114, 2020.
22. Livak KJ and Schmittgen TD: Analysis of relative gene expression data using real-time quantitative PCR and the 2(-Delta Delta C(T)) method. Methods 25: 402-408, 2001.
23. Kuprash DV and Nedospasov SA: Molecular and cellular mechanisms of inflammation. Biochemistry (Mosc) 81: 1237-1239, 2016.
24. Chen B, Ma Y, Xue X, Wei J, Hu G and Lin Y: Tetramethylpyrazine reduces inflammation in the livers of mice fed a high fat diet. Mol Med Rep 19: 2561-2568, 2019.
25. Sayers SR, Beavil RL, Fine NHF, Huang GC, Choudhary P, Pacholarz KJ, Barran PE, Butterworth S, Mills CE, Cruickshank JK, *et al*: Structure-functional changes in eNAMPT at high concentrations mediate mouse and human beta cell dysfunction in type 2 diabetes. Diabetologia 63: 313-323, 2020.
26. Lassailly G, Bou Saleh M, Leleu-Chavain N, Ningarhari M, Gantier E, Carpentier R, Artru F, Gnemmi V, Bertin B, Maboudou P, *et al*: Nucleotide-binding oligomerization domain 1 (NOD1) modulates liver ischemia reperfusion through the expression adhesion molecules. J Hepatol 70: 1159-1169, 2019.
27. Wolfrum C, Poy MN and Stoffel M: Apolipoprotein M is required for prebeta-HDL formation and cholesterol efflux to HDL and protects against atherosclerosis. Nat Med 11: 418-422, 2005.
28. Adib-Conquy M and Cavaillon JM: Host inflammatory and anti-inflammatory response during sepsis. Pathol Biol (Paris) 60: 306-313, 2012 (In French).
29. Scheller J, Chalaris A, Schmidt-Arras D and Rose-John S: The pro- and anti-inflammatory properties of the cytokine interleukin-6. Biochim Biophys Acta 1813: 878-888, 2011.
30. Iyer SS and Cheng G: Role of interleukin 10 transcriptional regulation in inflammation and autoimmune disease. Crit Rev Immunol 32: 23-63, 2012.
31. Baeck C and Tacke F: Balance of inflammatory pathways and interplay of immune cells in the liver during homeostasis and injury. EXCLI J 13: 67-81, 2014.
32. Ben-Neriah Y and Karin M: Inflammation meets cancer, with NF-κB as the matchmaker. Nat Immunol 12: 715-723, 2011.
33. Ma X, Hu YW, Zhao ZL, Zheng L, Qiu YR, Huang JL, Wu XJ, Mao XR, Yang J, Zhao JY, *et al*: Anti-inflammatory effects of propofol are mediated by apolipoprotein M in a hepatocyte nuclear factor-1α-dependent manner. Arch Biochem Biophys 533: 1-10, 2013.
34. Galvani S, Sanson M, Blaho VA, Swendeman SL, Obinata H, Conger H, Dahlbäck B, Kono M, Proia RL, Smith JD and Hla T: HDL-bound sphingosine 1-phosphate acts as a biased agonist for the endothelial cell receptor S1P1 to limit vascular inflammation. Sci Signal 8: ra79, 2015.
35. Zheng Z, Zeng Y, Zhu X, Tan Y, Li Y, Li Q and Yi G: ApoM-S1P modulates Ox-LDL-induced inflammation through the PI3K/Akt signaling pathway in HUVECs. Inflammation 42: 606-617, 2019.
36. Mierzejewska P, Zabielska MA, Kutryb-Zajac B, Tomczyk M, Koszalka P, Smolenski RT and Slominska EM: Impaired L-arginine metabolism marks endothelial dysfunction in CD73-deficient mice. Mol Cell Biochem 458: 133-142, 2019.
37. Li F, Zhang T, He Y, Gu W, Yang X, Zhao R and Yu J: Inflammation inhibition and gut microbiota regulation by TSG to combat atherosclerosis in ApoE(-/-) mice. J Ethnopharmacol 247: 112232, 2020.